ARTICLE

Check for updates

Severity of neonatal influenza infection is driven by type I interferon and oxidative stress

Ogan K. Kumova[1,7], Ioanna-Evdokia Galani[2], Abhishek Rao[1], Hannah Johnson[3], Vasiliki Triantafyllia[2], Stephanie M. Matt[3], Judy Pascasio[4], Peter J. Gaskill[3], Evangelos Andreakos[2], Peter D. Katsikis[5] and Alison J. Carey[1,6]✉

© The Author(s), under exclusive licence to Society for Mucosal Immunology 2022

Neonates exhibit increased susceptibility to respiratory viral infections, attributed to inflammation at the developing pulmonary air-blood interface. IFN I are antiviral cytokines critical to control viral replication, but also promote inflammation. Previously, we established a neonatal murine influenza virus (IV) model, which demonstrates increased mortality. Here, we sought to determine the role of IFN I in this increased mortality. We found that three-day-old IFNAR-deficient mice are highly protected from IV-induced mortality. In addition, exposure to IFNβ 24 h post IV infection accelerated death in WT neonatal animals but did not impact adult mortality. In contrast, IFN IIIs are protective to neonatal mice. IFNβ induced an oxidative stress imbalance specifically in primary neonatal IV-infected pulmonary type II epithelial cells (TIIEC), not in adult TIIECs. Moreover, neonates did not have an infection-induced increase in antioxidants, including a key antioxidant, superoxide dismutase 3, as compared to adults. Importantly, antioxidant treatment rescued IV-infected neonatal mice, but had no impact on adult morbidity. We propose that IFN I exacerbate an oxidative stress imbalance in the neonate because of IFN I-induced pulmonary TIIEC ROS production coupled with developmentally regulated, defective antioxidant production in response to IV infection. This age-specific imbalance contributes to mortality after respiratory infections in this vulnerable population.

Mucosal Immunology (2022) 15:1309–1320; https://doi.org/10.1038/s41385-022-00576-x

INTRODUCTION

Neonates less than six months of age, especially preterm neonates, are particularly susceptible to respiratory tract infections[1]. Morbidity and mortality associated with these infections are inversely correlated with age, with the highest susceptibility during the first few months of life[2]. Although this susceptibility to respiratory viral infections has been attributed to the immunological immaturity of the newborn[3,4], the underlying mechanisms are poorly understood. The neonatal immune system evolves during the transition from fetal to *ex utero* life. There are quantitative and qualitative differences in immune cells, cytokines, and antibodies compared to adults[5] which contribute to respiratory viral susceptibility[6]. Poorly regulated innate immune responses can be more damaging during infection[7,8].

A key part of these innate immune responses to viral infection is the production of type I interferons, mainly, IFNα/β[9]. These cytokines are produced by various immune and parenchymal cell types upon viral infection to reduce viral replication and activate subsequent immune responses[10]. However, a more pathogenic role of IFNα/β has recently been highlighted in the brain of HSV-1 infected neonates[8,11]. There are inconsistencies in the literature about whether respiratory viral infection-stimulated IFNα/β is deleterious[12–14] or protective[15–18]. Induction of IFNα/β is followed by production of inflammatory cytokines and chemokines which leads to recruitment of immune cells and bystander damage.

In addition to pulmonary type I interferons, type III interferons (IFNλ, IL-28A/B, IL-29) play an important early protective role in influenza virus infection because they limit viral replication and spread from the upper airway to the lower respiratory tract[19] without causing inflammation in the airways[20]. IFNλ have a similar expression pattern, function[21], and homology to type I interferons[22].

Respiratory viruses such as influenza and respiratory syncytial virus (RSV) generate reactive oxygen species (ROS) in infected cells and induce oxidative stress[23–25] to aid in their replication. Increases in ROS and oxidative stress imbalance are coupled with the progression of viral diseases and contribute to influenza-mediated lung damage[23,26,27]. In viral hepatitis, type I interferon-mediated oxidative stress has a direct effect on liver damage[28]. However, this direct link has not yet been established in pulmonary infection with respiratory viruses. Newborns, especially preterm neonates are particularly vulnerable to the deleterious effects of ROS and oxidative stress, as they lack adequate pulmonary antioxidant levels[29–32].

Previously, we demonstrated that neonatal mice are extremely susceptible to influenza virus[33,34]. We hypothesize here

[1]Microbiology and Immunology, Drexel University College of Medicine, Philadelphia, PA, USA. [2]Laboratory of Immunobiology, Center for Clinical, Experimental Surgery and Translational Research, Biomedical Research Foundation Academy of Athens, Athens, Greece. [3]Pharmacology and Physiology, Drexel University College of Medicine, Philadelphia, PA, USA. [4]Pathology, Drexel University College of Medicine, Philadelphia, PA, USA. [5]Immunology, Erasmus University Medical Center, Rotterdam, the Netherlands. [6]Pediatrics, Drexel University College of Medicine, Philadelphia, PA, USA. [7]Present address: U.S. Food and Drug Administration, Center for Biologics Evaluation and Research, Silver Spring, MD, USA. ✉email: ajc327@drexel.edu

Received: 26 October 2021 Revised: 26 September 2022 Accepted: 23 October 2022
Published online: 9 November 2022

that influenza virus-induced IFNα/β has a direct role in this susceptibility. To test this hypothesis, we used our in vivo neonatal mouse model and primary neonatal respiratory epithelial cells to examine the direct impact of Type I IFNs on ROS production and oxidative stress. Here, we delineate the pathogenic role of IFNβ-mediated oxidative stress in the neonatal lung during an acute influenza infection and demonstrate the therapeutic value of antioxidant treatment during neonatal infection.

RESULTS

Deletion of IFNαβR rescues influenza virus-mediated mortality

Three-day-old mice are exquisitely sensitive to influenza virus (IV) infection and exhibit high mortality[33]. Most pups die between 6 and 8 days post infection, which suggests a defective or pathogenic early neonatal antiviral immune response. Type I interferons (IFN I) are key antiviral cytokines produced during early infection and grant viral resistance to uninfected cells[17,35]. We hypothesized that neonates had a defective IFN I response, which contributed to increased early mortality. To assess the contribution of IFN I during neonatal IV infection, we utilized IFNαβR deficient mice, which are unable to respond to IFN I, including IFNα and IFNβ, the most common IFN I. Three-day-old IFNαβR$^{-/-}$ and aged-matched C57BL/6 (WT) neonates were infected with the H1N1 strain PR8 (A/Puerto Rico/8/34) influenza A virus and tracked for survival. Next, we independently confirmed these findings in a different animal housing location to avoid microbiome effects that may impact reproducibility of data[36]. Strikingly, two independent labs demonstrated IFNαβR$^{-/-}$ neonatal mice had an improved average survival rate of 70% compared to 13% survival in wild-type (WT) neonatal mice (Fig. 1a**)**.

In contrast to our finding with murine neonates, absence of IFNαβR in adults is deleterious[20]. To confirm these previous findings, IFNαβR$^{-/-}$ and WT adults were infected with H1N1 strain PR8 (A/Puerto Rico/8/34) influenza A virus and tracked for weight loss, an indicator of morbidity. IFNαβR$^{-/-}$ adults lost on average 33% of their initial body weight, compared to 20% in the WT adult mice, and failed to recover their initial body weight as quickly during IV infection (Fig. 1b). We next questioned if IFNαβR$^{-/-}$ neonates had differences in their viral loads. Consistent with the literature[15,37], viral titers at early points of infection (1-, 3-, and 6-days post-infection) were comparable between the wild-type WT and IFNαβR$^{-/-}$ neonates (Fig. 1c).

IFNλ is essential to protect neonatal mice during influenza virus infection

Due to their overlapping functions with IFN I, we questioned if deletion of IFNλ receptor (Ifnlr1 or IL28Rα) would have a similar protective effect as deletion of IFNαβR$^{-/-}$. Three-day-old Ifnlr $^{-/-}$ and aged-matched WT neonates were infected with the same H1N1 strain PR8 (A/Puerto Rico/8/34) influenza A virus and tracked for survival. Compared to wild-type neonatal mice with 15% survival, Ifnlr1$^{-/-}$ neonates all succumbed to infection (Fig. 1d). Next, viral loads were assessed in Ifnlr1$^{-/-}$ neonates. Lungs were harvested from Ifnlr1$^{-/-}$ and WT neonates at 1-, 3- and 6-days post-infection. There were no differences in viral burden in the lungs at these time points (Fig. 1e).

To determine the dominant interferon, Type I or III, in the protection or susceptibility of murine neonates to IV, animals deficient in both IFNαβR and Ifnlr1 were created, termed IFNαβR$^{-/-}$ Ifnlr1$^{-/-}$. Three-day-old IFNαβR$^{-/-}$ Ifnlr1$^{-/-}$ and age-matched WT neonatal mice were infected and tracked for survival. Both the wild type and IFNαβR$^{-/-}$ Ifnlr1$^{-/-}$ neonates had similar survival levels with all neonates succumbing to the infection by day 10 (Fig. 1d). These results suggest that IFNλ plays an indispensable protective role in the neonates during IV infection without compromising the host fitness, especially in early life.

IFNβ administration post-influenza infection accelerates death in neonates

Administration of recombinant IFNβ prior to neonatal IV infection protects from mortality[33,38,39]. However, based on the improved survival of IFNαβR$^{-/-}$ neonatal mice after IV infection (Fig. 1a), we sought to determine if administration of IFNβ after the infection would be deleterious to the murine neonates. Three-day-old neonatal mice were infected with the same influenza virus strain as above and treated 24 h post infection with 1000U recombinant mouse IFNβ or sterile 0.9% saline intranasally (Fig. 2a). IFNβ treatment post infection accelerated neonatal death, with 95% mortality by 5 days post infection (Fig. 2b, black solid line), compared to infected neonatal mice treated with saline, with 75% mortality (Fig. 2b, black dashed line). Adult mice treated with 4000U units of IFNβ 24 h post infection had no associated mortality (Fig. 2b, red dashed line). In contrast to infected neonates, IFNβ treatment had no effect on survival of age-matched uninfected neonates (Fig. 2b, green dashed line). Previously, we demonstrated that neonates have a delayed upregulation of interferon stimulated genes (ISG) in influenza viral infection[33] and others have demonstrated this with RSV infection[40]. Surprisingly, no differences in IFNβ transcription were found between WT neonates and adults at 1- or 3-days post-infection, which suggests that neonates have an aberrant interferon stimulation pathway which increases sensitivity to IFNβ effects, compared to adults (Supplementary Fig. 1). Together, these data confirm an age-specific deleterious effect of IFNβ during neonatal IV infection.

Improved pulmonary pathology in IFNαβR deficient animals

Due to the improved survival of IFNαβR$^{-/-}$ neonatal mice, we asked if lung pathology was improved in IFNαβR$^{-/-}$ infected mice. Lung histopathology from IFNαβR$^{-/-}$ neonates was compared to age-matched WT neonates using a weighted scoring system[33]. This scoring method accounts for the percentage of lung affected, in addition to the severity of alveolitis and peribronchiolitis. The scoring was performed by a pathologist blinded to the genotype of the neonates. Three-day-old IFNαβR$^{-/-}$ and WT neonates were infected as above. Although early pathology scores did not differ between the WT and IFNαβR$^{-/-}$ mice, severity scores increased significantly in WT neonates at 6-days post-infection, compared to IFNαβR$^{-/-}$ neonates (Fig. 2c). While IFNαβR$^{-/-}$ neonates had small areas of affected lung, the WT mice had large sections of affected lung, which demonstrated septal wall thickening with cellular infiltration and alveolitis (Fig. 2d). Therefore, neonatal mice deficient in type I IFN signaling had improved lung pathology at 6-days post-IV infection, when WT mice mortality begins (Fig. 1a), which demonstrates a pathogenic role of type I IFN in neonatal mouse IV infection.

IFNαβR deficient animals have differential immune cell recruitment during early infection

In IV-infected adult mice, high amounts of IFN I correlate with increased recruitment and proliferation of inflammatory monocytes and subsequent immunopathogenesis[41,42]. We asked whether loss of IFN I signal in the neonate would decrease recruitment of inflammatory monocytes to the alveolar airspace and the lung interstitium. Three-day-old IFNαβR$^{-/-}$ and WT neonates were infected with IV. Bronchoalveolar lavage fluid and whole lung tissue was collected at 1- and 3-days post-infection. We found no differences in total cell count in the BAL or the lung at 1-day post-infection (Supplementary Fig. 2a, b**)**. However, there was a significant decrease in total cells in the BAL in IFNαβR$^{-/-}$ neonates at 3 days post infection, relative to WT neonates. Inflammatory monocytes (CD11b^{hi}, Ly6C^{hi}, Ly6G^{-}, MHC II^{+}) and neutrophils (CD11b^{hi}, Ly6C^{-}, Ly6G^{+}) were defined based on Terrazas, et al.[43] (Supplementary Fig. 3). Inflammatory monocytes and neutrophils were significantly decreased in the BAL but not in the lung interstitium at 1- and 3-days post-infection in IFNαβR$^{-/-}$ neonates compared to WT neonates

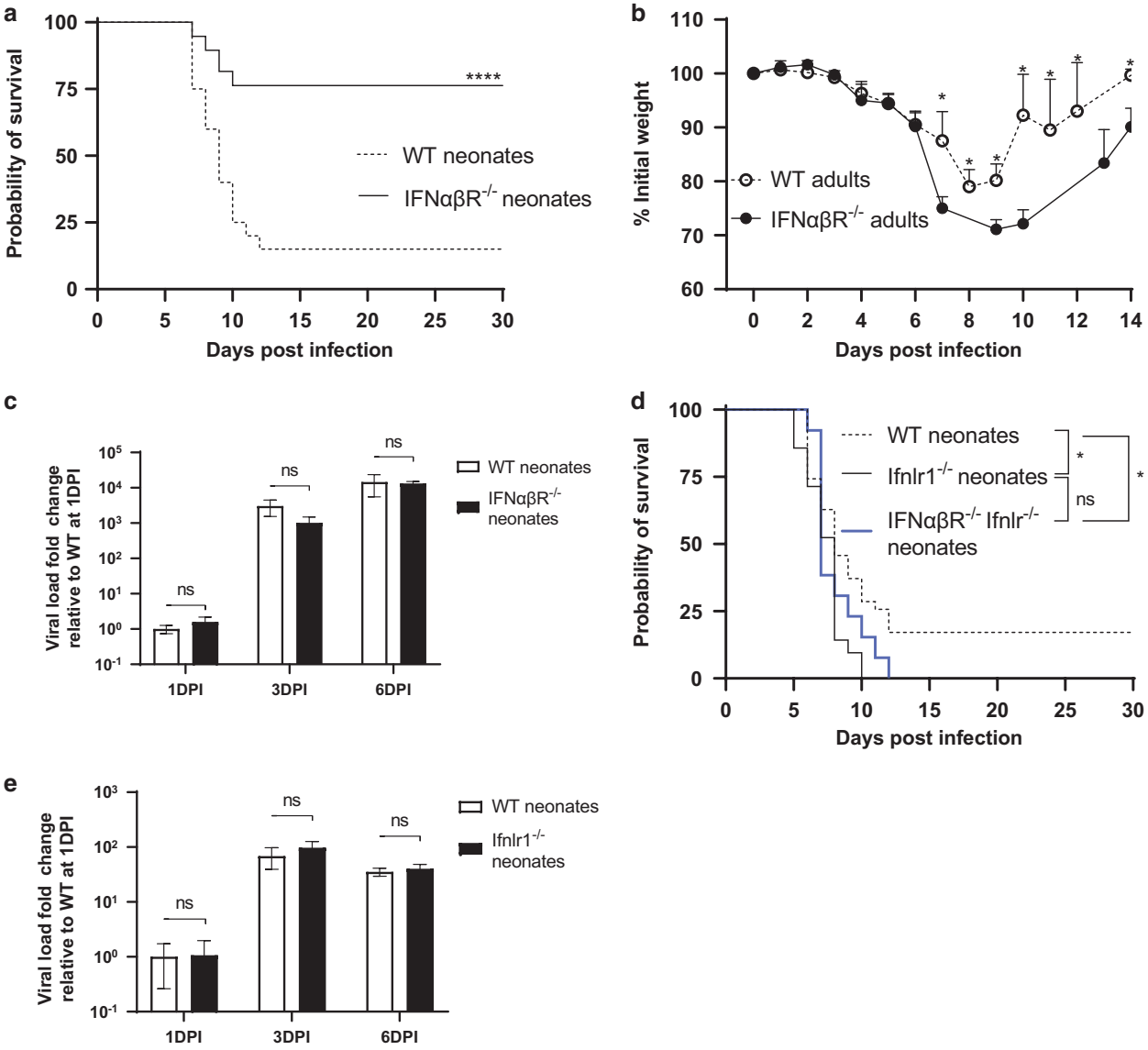

Fig. 1 Type I interferons are deleterious during neonatal influenza virus infection, while type III interferons are essential to protection. Three-day old neonatal and 8-week-old adult mice were intranasally infected with PR8 influenza A virus. **a** Wild-type (dashed line) ($n = 31$) and IFNαβR$^{-/-}$ (solid line) ($n = 46$) neonates were infected and tracked for survival (5 total independent experiments at 2 separate vivarium, 3 experiments performed at Drexel University (DU) and 2 experiments performed at Biomedical Research Foundation Academy of Athens(BRFAA) **b** At DU, 8-week-old wild-type (open circle) ($n = 12$, 3 independent experiments) and IFNαβR$^{-/-}$ (closed circle) ($n = 15$, 4 independent experiments) mice were intranasally infected with PR8 influenza A virus and weights were tracked. Viral burden was determined at 1-, 3-, and 6- days post-infection by real-time PCR and is reported as the fold change relative to a 1-day post-infection wild-type neonatal mouse for **c** IFNαβR$^{-/-}$ and **e** Ifnlr1$^{-/-}$ neonatal mice. **d** At BRFAA, wild-type (dashed line) ($n = 9$, 2 separate experiments) and Ifnlr1$^{-/-}$ (black line) ($n = 12$, 2 independent experiments) and IFNαβR$^{-/-}$ Ifnlr1$^{-/-}$ (blue line) ($n = 14$, 2 independent experiments) neonates were infected and tracked for survival. For viral load analysis, protocol 1 was used for IFNαβR$^{-/-}$ at DU and protocol 2 was used for Ifnlr1$^{-/-}$ at BRFAA. Statistical differences between wild type and transgenic animal survival were assessed by using log-rank (Mantel–Cox) test and Mann-Whitney test when comparing nonparametric values for viral loads and weight loss, where denoted *$p < 0.05$, ****$p < 0.0001$.

(Fig. 2e, g, Supplementary Fig. 4). There were no differences in macrophage (CD11b$^+$ F4/80$^+$) or classical dendritic cell (CD11b$^+$ and/or CD11c$^+$, MHC II^{hi})[44] numbers at the assessed time points (Fig. 2e–h). Therefore, IFN I drive enhanced recruitment of inflammatory monocytes and neutrophils into the airway during neonatal IV infection, directly impacting immunopathology.

IFNβ induces oxidative stress during neonatal influenza viral infection

IFN I prime cells to produce reactive oxygen species[45] during IV infection[46,47]. Inflammatory monocytes and neutrophils have an enhanced ability to produce ROS during infection and inflammation[23,48,49]. Based on increased recruitment of inflammatory cells into the alveolar airspace in neonates during IV infection, we next questioned whether these cells were under increased oxidative stress compared to their adult counterparts. To assess pulmonary oxidative stress during early stages of infection, neonatal and adult mice were infected with IV, and lungs were harvested 2-days post-infection. The whole lung cell suspension was treated with IFNβ ex vivo for an hour before measuring oxidative stress by CellROX. N-acetylcysteine (NAC) treated cells were used as background controls for both neonates and adults and yielded similar results (Supplementary Fig. 5a). Age-matched IV-infected animals treated with saline were used to provide a

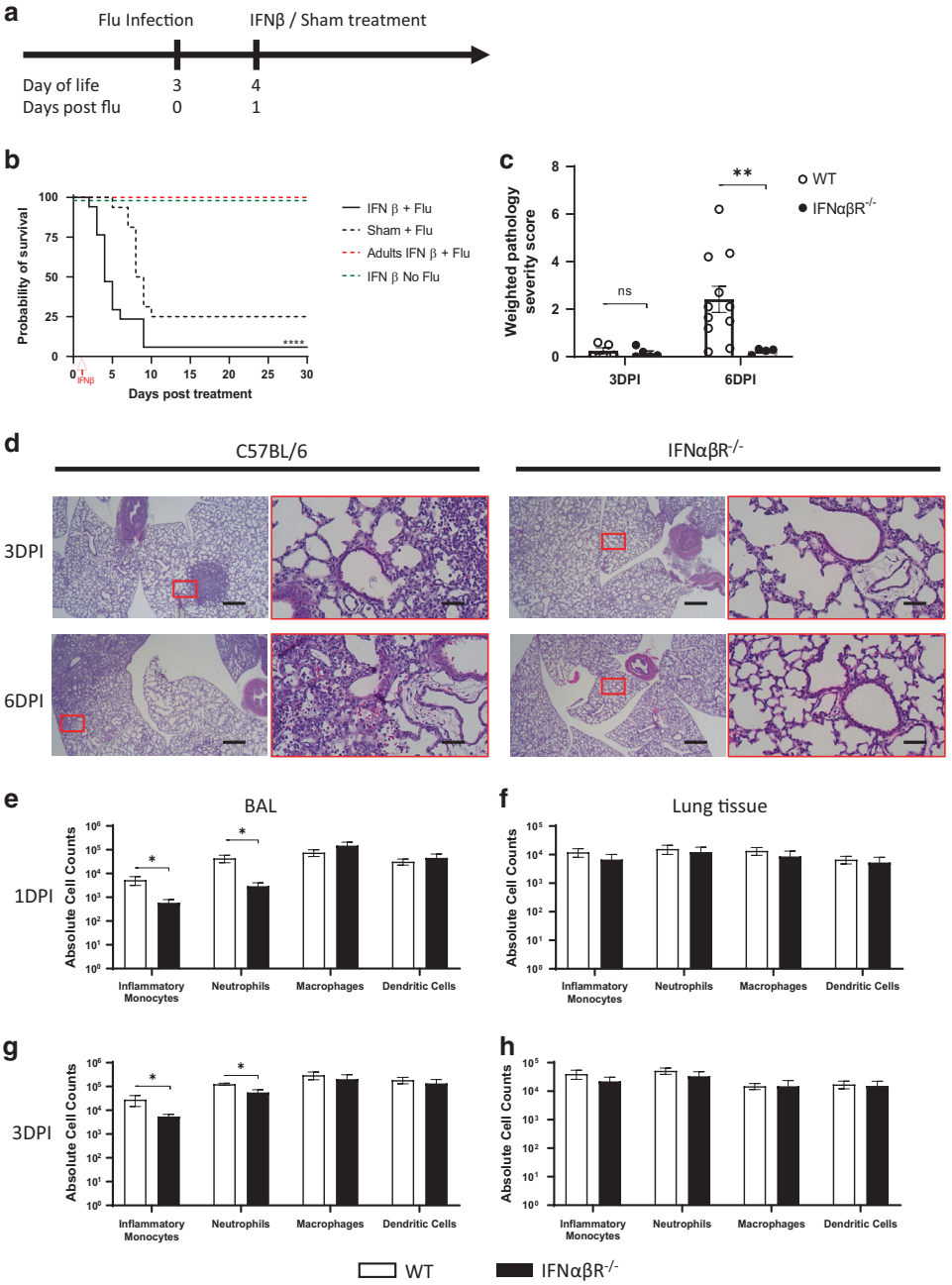

Fig. 2 Type I interferons accelerate mortality and worsen pathology after neonatal influenza virus infection. a, b Three-day-old and 8-week-old wild-type mice were intranasally infected with PR8 influenza A virus or saline. Recombinant IFNβ (1000 units for neonates or 4000 units for adults) or saline (sham) was administered 24 h post infection per the **a** experimental scheme and **b** survival was tracked. Infected neonates who received IFNβ treatment (black solid line, $n = 12$) are compared to sham-treated infected neonates (black dash line, $n = 11$), uninfected neonates with IFNβ treatment (green dashed line, $n = 8$) and infected adult mice with IFNβ treatment (red dash line, $n = 6$) (2–3 independent experiments). **c–h** In separate experiments, neonatal wild type and IFNαβR$^{-/-}$mice were infected at 3-days of age intranasally with PR8 influenza A virus. **c** Pathology severity scores were assessed at 3- and 6-days post-infection (3 independent experiments) ($n = 5$–11). **d** Representative images demonstrate increased alveolitis and peribronchiolitis in wild-type animals. Scale bar: 50 μm (High magnification) or 500 μm (Low magnification). Absolute cell counts of specified cell types per 100mg of lung was determined by flow cytometry in the **e, g** bronchoalveolar lavage and **f, h** interstitial lung at 1- **e, f** and 3-days post-infection **g, h** (2 independent experiments, $n = 4$–6). Statistical differences between wild type and IFNβ treatmentsurvival were assessed by using log-rank (Mantel–Cox) test. Student's *T* test was used when comparing 2 roups for pathology severity scores and immunophenotyping, where denoted *$p < 0.05$, **$p < 0.01$, ****$p < 0.0001$.

baseline to compare to those animals treated with IFNβ. There was increased oxidative stress in inflammatory monocytes, macrophages, and CD45$^-$ epithelial cells from infected neonatal animals, compared to adults, after ex vivo IFNβ treatment (Fig. 3a, Supplementary Fig. 5b). In addition, the CD45$^-$ epithelial cell population had the greatest fold increase (7.5-fold) in oxidative stress relative to adults.

To directly assess the relative contribution of superoxide production to the oxidative stress imbalance, we employed dihydroethidium (DHE) staining coupled to multicolor flow

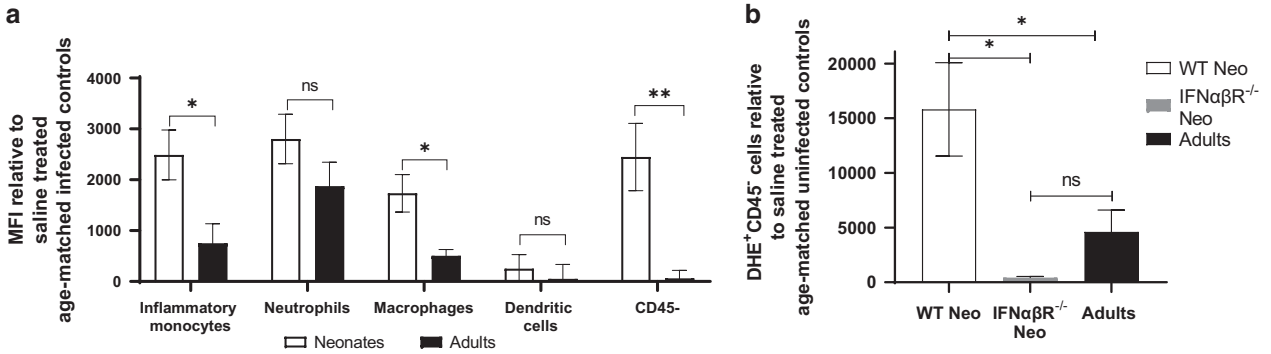

Fig. 3 Neonates have increased oxidative stress and reactive oxygen species production following influenza viral infection. To determine oxidative stress and reactive oxygen species production in the infected neonate versus adult, 3-day-old neonatal and 8-week-old adult mice were intranasally infected with PR8 influenza A virus. Mice were harvested 2-days post-infection. **a** Oxidative stress imbalance was determined with CellROX staining after the infected whole lung cell suspension was treated with IFNβ or saline (control), ex vivo for an hour. Average mean fluorescence intensity (MFI) of CellROX in the specified immune cell populations in neonates (white bars) ($n = 7$, 2 independent experiments) and adults (black bars) post-IFNβ treatment ($n = 6$, 2 independent experiments). **b** To quantify ROS production in neonates versus adults, dihydroethidium staining was performed. Two days post infection, the whole lung cell suspension was treated with IFNβ or saline (control), ex vivo for an hour. The number of DHE^{+} $CD45^{-}$ cells post-IFNβ treatment is compared to age-matched saline treated uninfected controls for WT neonates (white bar), $IFN\alpha\beta R^{-/-}$ neonates (gray bar), and adults (black bar) ($n = 5$–6 in each group, 2 experiments). Statistical differences between groups were assessed using Mann–Whitney test when comparing 2 groups for MFI and absolute cell count differences, where denoted *$p < 0.05$, **$p < 0.01$.

cytometry. DHE can directly measure the amount of ROS in live cells with specificity for superoxide and hydrogen peroxide[50]. Again, neonatal and adult mice were infected with IV, and lungs were harvested 2-days post-infection. Whole lung suspensions were treated as above and the cells were stained with DHE following multicolor conjugated antibody application. There was no difference in ROS production in immune cell types in the presence of IFNβ compared to infected adults (Supplementary Fig. 6). To specifically investigate the impact of type I interferons on ROS production in $CD45^{-}$ epithelial cells, infected neonatal wild type and $IFN\alpha\beta R^{-/-}$ and adult wild-type mouse lung suspensions were compared to uninfected age-matched controls. Wild-type neonates had a significant increase in ROS production by $CD45^{-}$ cells, as compared to $IFN\alpha\beta R^{-/-}$ neonates and wild-type adults, relative to uninfected controls (Fig. 3b, Supplementary Fig. 7). Therefore, this suggests infected neonatal epithelial cells are particularly sensitive to IFNβ exposure and have a higher propensity to produce ROS in response to IFNβ.

Influenza infection is required for IFN I mediated oxidative stress imbalance in neonatal Type II pulmonary epithelial cells

Based on epithelial cells ($CD45^{-}$) having increased ROS based on DHE staining compared to adult controls, we sought to identify whether type II pulmonary epithelial cells (TIIEC) were a key source of oxidative stress, as the IV replication cycle contributes to production of ROS by infected epithelial cells[51]. TIIEC are a primary target for IV infection and play an important role in mounting an initial response to the infection[52,53]. We optimized TIIEC isolation methods[54,55] to establish a biologically relevant ex vivo neonatal lung epithelial cell platform. TIIEC are approximately 85% pure after the isolation, based on flow cytometry (Supplementary Fig. 8).

Neonatal and adult mice were infected in vivo and TIIEC were harvested 2-days post-infection, with uninfected, aged-matched animals as controls. To examine whether there was increased oxidative stress in influenza virus-infected TIIEC in response to IFNβ, cells were untreated or treated with IFNβ or tert-Butyl hydroperoxide (TBHP), a known inducer of ROS, ex vivo for an hour before measuring oxidative stress with CellROX. Infected neonatal and adult TIIEC were evaluated with the CellInsight CX7 high content screening platform. This confocal imaging system allows automated, unbiased confocal microscopic analysis of large numbers of individual cells across a population, enabling oxidative stress detection through CellROX staining to be evaluated at the individual cell level.

The TIIEC were co-stained with DAPI (blue), WGA (red) and CellROX to measure oxidative stress (green) (Fig. 4a). There is not an increase in oxidative stress in the infected adult TIIEC with the ex vivo application of IFNβ (Fig. 4a, b). In contrast, infected neonatal animals exhibited increased oxidative stress in response to exogenous ex vivo IFNβ treatment, compared to untreated neonatal cells and adult cells (Fig. 4a, b). Next, we sought to determine if this oxidative stress was specific to IV infection or was solely developmentally associated. Importantly, we detected over a 2-fold increase in oxidative stress by infected neonatal TIIEC compared to uninfected neonates (Fig. 4c). Together, these data indicate that infected neonatal TIIEC had increased oxidative stress upon exposure to IFNβ compared to infected adults and uninfected neonates based on high content screening.

Next, to confirm the pivotal role of type I interferons in oxidative stress imbalance, infected neonatal wild type and $IFN\alpha\beta R^{-/-}$ TIIEC were isolated and treated as above. Flow cytometric analysis of CellROX staining was performed. $IFN\alpha\beta R^{-/-}$ neonates did not display a significant increase in oxidative stress (Fig. 4d). Therefore, neonatal influenza viral infection coupled with IFN I programs oxidative stress, a feature not found in uninfected neonates and infected adults.

Neonates fail to upregulate antioxidant enzymes during infection

Neonates, especially premature neonates, are more prone to oxidative stress as they move from an oxygen poor *in utero* environment to oxygen rich *ex utero* environment[56,57] and lack robust antioxidant systems[58]. During IV infection[59] and other lung diseases, antioxidant enzymes are upregulated and shuttled to the extracellular matrix[60]. Potentially, the neonatal propensity towards oxidative stress during IV infection (Fig. 4c) could be due to an aberrant antioxidant response, coupled with increased ROS (Fig. 3b). Therefore, we hypothesized neonatal mice would not respond to IV infection with an increase in these antioxidant enzymes. Superoxide dismutase 3 (SOD3) (Fig. 5a), glutathione peroxidase 3 (GPX3) (Fig. 5b), glutathione synthetase (GSS) (Fig. 5c), and peroxiredoxin 1 (PRDX1) (Fig. 5d) transcripts were analyzed in murine lungs from IV-infected wild-type neonates, $IFN\alpha\beta R^{-/-}$ neonates, and adults, as well as from uninfected animals. In response to IV infection, adult mice increase transcription of antioxidant enzymes between 1- and 3-days post-infection, compared to their age-matched uninfected counterparts (Fig. 5a–d). In contrast, both IV-infected wild-type and $IFN\alpha\beta R^{-/-}$ neonates fail to upregulate these enzymes during

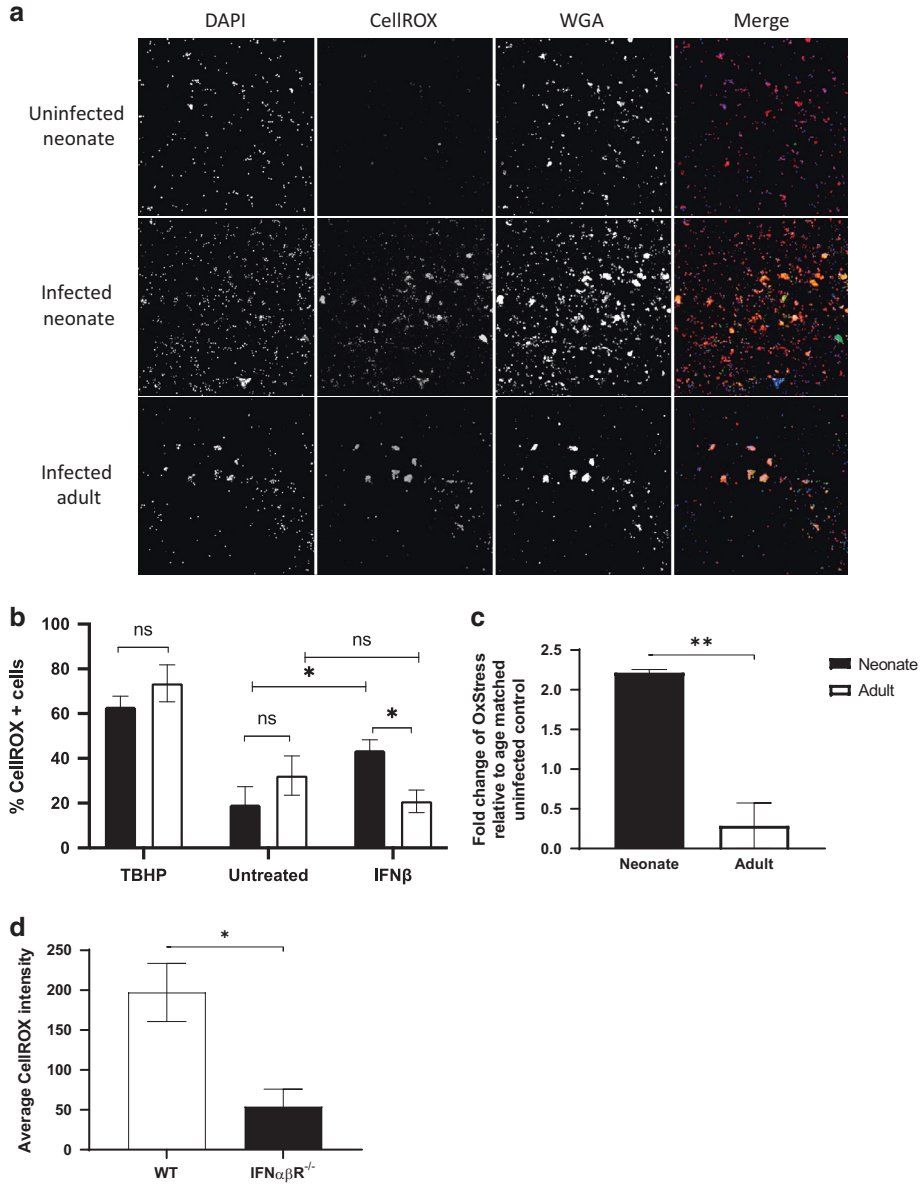

Fig. 4 Influenza-infected neonates have greater oxidative stress imbalance in response to IFNβ. Three-day-old neonatal and 8-week-old adult WT mice were intranasally infected with PR8 influenza A virus. Age-matched uninfected mice were used as controls. Mice were harvested 2-days post-infection and Type II epithelial cells were isolated. The TIIEC were treated with an antioxidant N-acetylcysteine (NAC), IFNβ, or tert-Butyl hydroperoxide (TBHP), or media (Untreated) ex vivo for an hour. NAC treated wells were used as background staining controls. The CellInsight CX7 high content screening platform was used to quantify CellROX intensity at the individual cell level. **a** Representative images at 10X magnification from IFNβ-treated uninfected and infected neonates and IFNβ-treated infected adults are depicted. The TIIEC were co-stained with DAPI (blue), WGA (red) and CellROX (green). **b** The percentage of CellROX positive cells relative to total cells in each treatment group is indicated. **c** Fold change of CellROX intensity relative to age-matched uninfected animals. $n = 9$ in neonates, $n = 3$ in adults, 3 independent experiments. To confirm the role of IFNβ in the neonatal program of oxidative stress imbalance during influenza virus infection, IFNαβR$^{-/-}$ and WT neonates were infected as above and TIIEC were harvested 2-days post-infection. **d** Relative fluorescence units of average CellROX intensity by flow cytometry in IFNβ-treated WT (white bar) and IFNαβR$^{-/-}$ neonates (black bar) is shown. Statistical differences between groups were assessed using Student's T test was used when comparing 2 groups, where denoted *$p < 0.05$, **$p < 0.01$.

infection. Therefore, IFN I do not play a suppressive role in antioxidant mechanisms; rather antioxidant gene transcription is developmentally-dependent. Moreover, IV-infected wild-type and IFNαβR$^{-/-}$ neonates at 1-day post-infection *suppressed* transcription of the extracellular enzyme SOD3, compared to the adult at 1-day post-infection (Fig. 5a). SOD3 is a key antioxidant enzyme in the alveolar airspace[59,61,62]. Therefore, neonates have a decreased ability to neutralize ROS in the alveolar airspace because of an age-dependent aberrant antioxidant response to influenza virus infection, compared to the adult increase in antioxidant production.

Antioxidant Treatment Rescues IFNβ mediated mortality in neonates, but not adults

Loss of SOD3 and GPX3 have been linked to tissue damage in the lung[62,63] and over-expression of SOD3 ameliorates lung pathology during IV infection[64]. Based on global increased oxidative stress during IV infection and IFNβ application, coupled with a defective antioxidant response during neonatal influenza viral infection, we asked if treatment with an antioxidant Acetadote would improve survival of IV-infected neonatal mice. Acetadote is a pharmaceutical grade N-acetylcysteine (NAC), used in the treatment of

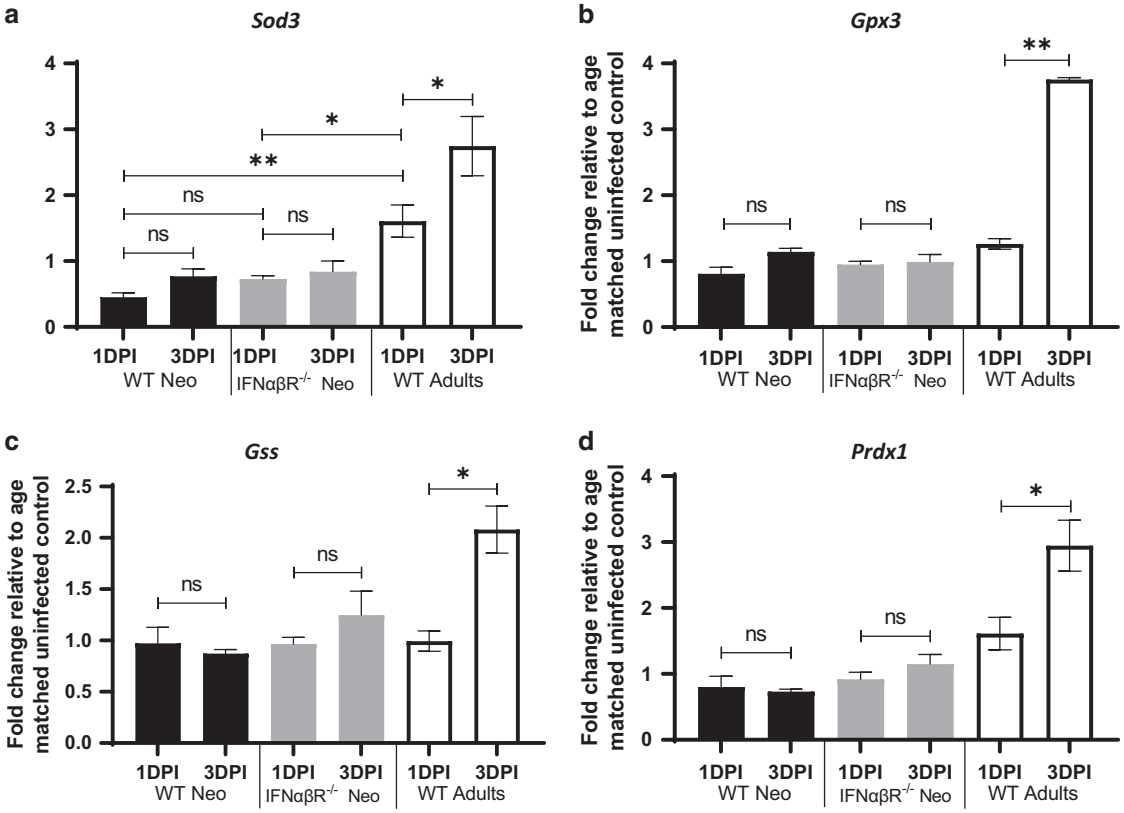

Fig. 5 Neonates fail to upregulate antioxidants during influenza virus infection. To determine changes in transcription of antioxidant enzymes in the infected animal, 3-day-old WT (black bars) and IFNαβR$^{-/-}$ (gray bars) neonatal and 8-week-old (white bars) mice were intranasally infected with PR8 influenza A virus. Lungs were harvested at 1- and 3-days post-infection, and from age-matched uninfected animals. **a** *Sod3*, **b** *Gpx3*, **c** *Gss*, and **d** *Prdx1* transcriptions were normalized to the housekeeping gene *gapdh* ($n = 3$–6 for each group). Data presented relative to uninfected age-matched mice. Data from 3 independent experiments. Statistical differences between groups were assessed sing one-way ANOVA to compare multiple groups, where denoted ns = non-significant, *$p < 0.05$, **$p < 0.01$.

acetaminophen overdose. Acetaminophen overdose significantly decreases intracellular glutathione, a major intracellular antioxidant. We administered 150 mg/kg of Acetadote intraperitoneally into neonatal mice on 1 and 2 days of age prior to IV infection at 3 days. Subsequent doses were given 1- and 3-days post-infection and the mice were tracked for survival (Fig. 6a). Neonatal mice treated with Acetadote had an improved survival (40%) during IV infection compared to their sham-treated litter mates (10%) (Fig. 6b). Next, we sought to determine if Acetadote treatment started post-infection could protect infected mice. Three-day old mice were infected and administered Acetadote intraperitoneally 1-, 3-, 5-, and 7-days post-IV infection (Fig. 6c). Neonatal mice receiving Acetadote had significantly improved survival (25%) compared to their sham recipient litter mates (10%) (Fig. 6d). In contrast, adults treated with the same weight-adjusted dose of 150 mg/kg NAC and pre-infection dosing schedule (Fig. 6e) do not show improve disease pathology (25% maximum weight loss) relative to PBS treated age-matched animals (21% maximum weight loss) (Fig. 6f). These data suggest that ROS production during neonatal infection contributes to pathogenicity, and that antioxidants are a possible therapeutic strategy during IV infection in this vulnerable population.

DISCUSSION

With an age-appropriate in vivo murine model of IV infection, our studies provide evidence that type I interferons directly promote an oxidative stress imbalance during IV infection. Neonates, especially premature neonates, are exquisitely sensitive to the pathogenic effects of ROS as they lack appropriate antioxidants in their lungs[29–32]. Here, we demonstrate an aberrant global antioxidant response to IV infection in murine neonates and increased pulmonary epithelial cell ROS production in response to IFNβ, which drives this oxidative stress imbalance. Importantly, exogenous antioxidant therapy partially rescues the IV-infected murine neonates, while there is no benefit to adult morbidity. ROS production is important for viral ribonucleoprotein nuclear export and viral release during respiratory viral infections[24,25,51,65] which contributes to damage in the lung tissue[47]. Blocking ROS production ameliorates viral replication, IV mediated inflammation[46], and lung damage. ROS produced by NADPH Oxidase (Nox) enzymes of both lung infiltrating immune cells and the lung epithelial cells can also contribute to lung injury and death either directly or via inflammatory cytokine production[24,47].

Removal and detoxification of ROS is catalyzed by several type of antioxidants. Key pulmonary antioxidants are the superoxide dismutases[66] which contain 3 members: cytosolic SOD1, mitochondrial SOD2, and extracellular SOD3[66,67]. SOD1 and SOD2 are intracellular antioxidants which neutralize ROS produced as a result of metabolic activity[67]. SOD3 is particularly important because over-expression of SOD3 in type II alveolar epithelial cells (TIIECs) aids in lung development of neonatal mice[68], attenuates toxicity following hyperoxia[61], and prevents IV-induced lung damage[64]. Neutrophils and macrophages exposed to type I IFNs have a higher propensity to produce ROS via the STAT-1 pathway[45,69]. During a viral hepatitis infection, type I IFNs down-regulate SOD1 and increase ROS formation, leading to liver damage[28]. Functional blocking of IFNαβR in macrophages and hepatocytes reduced ROS generation and liver damage[28]. Consistent with this, IV-infected wild-type murine neonatal TIIECs

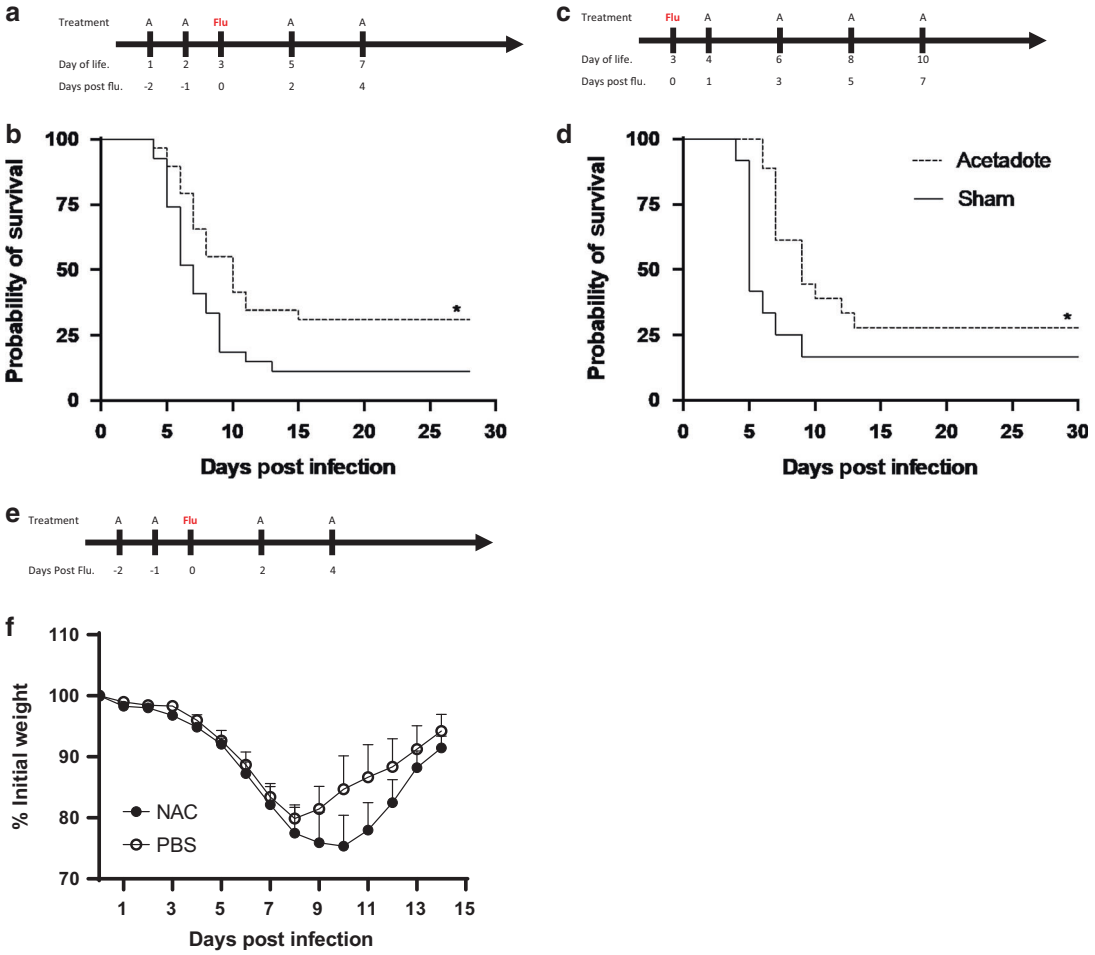

Fig. 6 Antioxidant treatment partially rescues neonates but not adults from influenza-mediated mortality. To determine if exogenous antioxidant could rescue neonatal and adult animals from oxidative stress imbalance-mediated mortality, animals were treated with 150 mg/kg of a pharmaceutical grade antioxidant, N-acetylcysteine (Acetadote) or sham at indicated time points **(a, c** and **e)** and tracked for survival (neonates, **b** and **d**) or weight loss (adults, **f**). Treatment with Acetadote partially rescues neonatal mice from influenza-mediated mortality when started prophylactically (**a** and **b**); Acetadote (dashed line) ($n = 29$), sham (solid line) ($n = 27$) 6 independent experiments. When Acetadote is started post-infection (**c** and **d**), there is improved survival; Acetadote (solid line) ($n = 18$), sham (dashed line) ($n = 9$) 4 independent experiments. In contrast, adults given the same weight-adjusted dose of NAC have no improvement in morbidity as demonstrated by similar weight loss kinetics (**b** and **f**), NAC (black circle) ($n = 5$, 3 males and 2 females), PBS (open circle) ($n = 5$, 3 males and 2 females), 2 independent experiments. Statistical differences between treated and control animals' survival on Kaplan Meier survival curve was assessed by using log-rank (Mantel–Cox) test, where denoted *$p < 0.05$, **$p < 0.01$.

produce ROS in response to IFNβ, in contrast to IFNαβR$^{-/-}$ murine neonatal TIIECs. Moreover, absence of ROS reduces lung damage and improves resolution of IV infection[70]. Here, both wild-type and IFNαβR$^{-/-}$ neonatal mice fail to upregulate several antioxidants in response to IV, as compared to their adult counterparts. These experiments provide strong evidence that the driver of the oxidative stress imbalance in wild-type animals is reactive oxygen species production in response to type I interferons.

Type I interferons (IFNα and IFNβ) induce an antiviral state, inhibit viral replication, and block the infection of neighboring cells[10,71]. Loss of function or mutation in type I interferons or their receptors increases symptom severity and mortality during viral infections in adult mice and humans[72,73]. Surprisingly, neonatal animals lacking the IFNα/β receptor are much more resistant to IV-related death relative to WT neonates, despite having similar viral burden. Type I interferons can act in an autocrine and paracrine manner, amplifying proinflammatory responses, which can lead to increased inflammation in the lung. There are inconsistencies in the literature about whether the IFN α/β produced in response to respiratory viral infection is deleterious[12–14] or protective[15–18], especially in neonates.

We speculate that the timing and magnitude of the neonatal IFN response is critical to whether it is deleterious or protective. For example, respiratory syncytial virus (RSV) induces poor IFN I, specifically IFNα, which contributes to RSV-mediated immunopathogenesis[74]. This reduction in IFN I during RSV is dependent on insulin-responsive aminopeptidase (IRAP) in alveolar macrophages[40] or hematopoietic growth factor ligand (Flt3-L) in DCs[75]. In contrast, we demonstrate IV induces similar IFN transcription in murine neonates compared to adults. However, consistent with others[40], previous work from our group revealed downstream IFN signaling and feedback is different in the IV-infected neonate, as ISGs are downregulated[33]. Finally, IFNβ prior to infection is protective, but induces rapid death if given after IV infection. Further investigation of the age-specific role of IFN I in different viral infections is warranted.

IFN I-induced oxidative stress is a critical mechanism of neonatal mortality during IV infection. IV infection programs neonatal immune and epithelial cells to have oxidative stress imbalance in response to IFN I. In contrast, ROS play an important role in IFN I regulation and are required for robust adult antiviral responses in epithelial cells[76]. Adult humans and mice lacking functional NOX2

complex leads to a prominent IFN I signature and higher inflammation with associated autoimmunity[77]. However, NOX2-mediated increase in ROS during RNA and DNA virus infections in endocytic compartments of monocytes and macrophages suppresses antiviral and humoral signaling[78]. Inhibition of NOX2-mediated ROS increase in these cell populations reduces IV-induced lung pathology[79]. In addition to amplification loops created by ROS, IFN I are responsible for increased recruitment of inflammatory monocytes which express Tumor necrosis factor (TNF)-related apoptosis-inducing ligand (TRAIL). Enhanced recruitment of $TRAIL^{+}$ inflammatory monocytes and increased expression of death-inducing receptor DR5 on epithelial cells has been linked to increased lung pathogenesis that is not present in $IFN\alpha\beta R^{-/-}$[13]. Together, these data indicate that type I IFNs could have a highly pathogenic role during neonatal IV infection.

Type III interferon (IFNλ, IL-28/29) has been identified as a non-redundant "front-line" antiviral interferon against IV and other respiratory viral infections[20]. While IFNλ signal through a distinct heterodimeric receptor, IFNλR1 (IL28Rα) and IL-10Rβ[80], similar signaling cascades to IFN-α/β are initiated, which results in overlapping interferon stimulated gene (ISG) expression[12]. IFNλ is the predominant early cytokine produced during IV infection[81] by respiratory epithelial cells and prevents the spread of virus from upper to lower airway[19]. WT and $IFN\alpha\beta R^{-/-}$ neonates have a similar viral burden, likely because IFNλ controls viral replication. IFNλ can maintain host fitness by creating a limited, protective inflammatory environment[20], which makes it indispensable during early IV infection in our neonatal murine IV model. IFNα, but not IFNλ, is deleterious when administered post-IV infection, and leads to increased inflammatory cytokines in BAL fluid and inflammatory monocyte frequency[14]. In addition, higher IFNλ levels in human infants correspond to improved clinical severity scores during early respiratory viral infection[82].

N-acetylcysteine has been proposed as a therapeutic for respiratory viral infections to combat oxidative stress. In addition to its mucolytic activity in the lung[83], it can directly scavenge oxygen free radicals via its thiol-reducing group, and indirectly aids in oxidative stress reduction by providing the necessary precursor cysteine for the synthesis of glutathione (GSH), a key intracellular antioxidant[84,85]. NAC attenuates pulmonary inflammation in adult BALB/c mice during H9N2 influenza infection. Adult animals that received NAC had lower amounts of proinflammatory cytokines in BAL[86]. Indeed, our short prophylactic treatment course with a pharmaceutical grade NAC provided protection to our neonates during IV infection, however NAC did not ameliorate IV infection-mediated weight loss in our adults. Importantly, NAC treatment begun 24 h post infection was protective. Recent studies have also confirmed that NAC has a direct inhibition effect on seasonal influenza viruses[87]. Therefore, antioxidants during IV infection are a promising therapeutic target specifically in the neonate population, both as a therapy to ameliorate oxidative stress and to limit IV replication.

Here, with a neonatal murine in vivo model of IV infection, we have challenged the paradigm of the protective role of IFN I and demonstrated age-specific developmental effects during IV infection. To our knowledge, this is the first study linking the neonatal type I interferon response to oxidative stress in the lung. We have demonstrated that the increase in ROS production in the neonatal mice is IFNβ mediated. Type III interferons can provide protection during a neonatal IV infection without IFN I's pathogenic side effects. In addition, ROS mediated mortality can be alleviated by administration of antioxidants both as a prophylactic and a therapeutic agent. This therapeutic potential takes advantage of the global, age-related aberrant antioxidant response to infection and thus, could potentially be applied to a broad range of viral infections.

METHODS

Mice, Infections, and Interferon β treatment

Eight-week-old adult C56BL/6J WT mice were purchased from Jackson Laboratory (Stock No: 000664-JAX) to use as adult controls and for in-house breeding. $IFN\alpha\beta R^{-/-}$ mice were purchased from Jackson Laboratories (Stock No: 32045-JAX) for in-house breeding. Experimental pups were obtained by timed mating in-house. The mice were housed under specific-pathogen-free conditions in an American Association for the Accreditation of Laboratory Animal Care (AAALAC)-certified barrier facility at both the Drexel University College of Medicine Queen Lane Campus and New College Building animal facilities.

Three-day-old neonatal mice (weight ~3 g) were infected intranasally (i.n.) with 0.12 $TCID_{50}$ (0.04 $TCID_{50}$/g) of influenza virus H1N1 strain PR8 (A/Puerto Rico/8/34) in a 5 µl volume. Adult 8-week-old WT mice (weight ~20 g) were infected i.n. with a sublethal dose of 3 $TCID_{50}$ in a 20 µl volume (0.15 $TCID_{50}$/g). The mice were anesthetized with inhaled isoflurane before intranasal inoculations. The pups were inspected daily for their activity level, respiratory rate, and the maternal interaction. If the pups were noted to be ignored or disregarded by the mother, had fast breathing, weight loss, or lack of movement when handled, they were removed from the cage. However, the majority of the pups did not exhibit signs of morbidity and were not found in the cage, assumed to be cannibalized by the mother.

Additionally, C57BL/6J WT (Stock No: 000664-JAX) and $IFN\alpha\beta R^{-/-}$ (Stock No: 32045-JAX) mice were both originally purchased from Jackson Laboratories, and $Ifnlr1^{-/-}$[81] mice on a C57BL/6J genetic background were bred at the Biomedical Research Foundation Academy of Athens (BRFAA) animal house, and their pups were obtained by timed mating. $IFN\alpha\beta R^{-/-}$ $Ifnlr1^{-/-}$ double knock-out animals were generated by breeding $IFN\alpha\beta R^{-/-}$ and $Ifnlr1^{-/-}$ until double knock-outs were achieved[20]. All mice were housed in specific-pathogen free (SPF) conditions in full compliance with Federation of Laboratory Animal Science Associations (FELASA) recommendations. All procedures had received approval from Institutional and Regional Ethical Review Boards. Three-day-old neonatal mice were infected intranasally (i.n.) with 3 pfu of influenza virus H1N1 strain PR8 (A/Puerto Rico/8/34) (Charles River Laboratories) in 5 µl volume under inhaled isoflurane anesthesia. Infectious viral load was determined by plaque assay of the titrated viral stock on MDCK cells.

Neonatal and adult mice were treated intranasally with 1000 or 4000 units of recombinant mouse Interferon β (Sigma-Aldrich, I9032), respectively. Recombinant IFNβ was diluted in normal saline to 200 units per µL; 5 µL for neonates or 20 µL for adults were administered intranasally under inhaled isoflurane anesthesia.

Viral loads

Protocol 1 (DU). At various time points post-infection, the lungs of the mice were harvested, weighed, and frozen at −80 °C in TRIzol (Invitrogen). RNA was isolated by the Qiagen RNeasy kit (Qiagen). The isolated RNA was then used for cDNA synthesis using the High-Capacity cDNA Reverse Transcription Kit (Applied Biosystems). Virus was measured by real-time PCR using influenza specific primers as previously described[88]. cDNA synthesis was performed using both a specific primer (5′-TCTAACCGAGGTCGAAACGTA-3′) and random hexamers. Real-time assays were performed in triplicate with 5 µl of cDNA, 12.5 µl of 2× TaqMan Universal PCR Master Mix (Applied Biosystems), 900 nM influenza A virus sense primer (5′-AAGACCAATCCTGTCACCTCTGA-3′), 900 nM influenza A virus antisense primer (5′-CAAAGCGTCTACGCTGCAGTCC-3′), and 200 nM influenza A virus probe (FAM-5′-TTTGTGTTCACGCTCACCGT-3′-TAMRA)[89]. All primers were specific for the influenza A virus matrix protein. Amplification and detection were performed using an Applied Biosystems Prism 7900HT sequence detection system with SDS 2.2.1 software (Applied Biosystems) at the following conditions: 2 min at 50 °C and 10 min at 95 °C, then 45 cycles of 15 s at 95 °C and 1 min at 60 °C. For viral load measurement, a standard curve was developed with serial 10-fold dilutions of stock PR8 with a known $TCID_{50}$ concentration. Ct values were plotted against virus quantity in $TCID_{50}$ per milliliter. This curve was used to convert the Ct values for viral loads to $TCID_{50}$ equivalents. Virus RNA quantities in lungs were expressed as fold change relative to age-matched 1-day post-infection neonatal mice.

Protocol 2 (BRFAA). At various time points post infection, the spleen and lung of the mice were harvested. The right lobes were weighed and snap-frozen in liquid nitrogen in TriReagent (Sigma-Aldrich) and placed in −80 °C for longer storage. The left lobes and the spleen were used for

FACS analysis. Frozen lungs were homogenized, and RNA isolation was performed through phase separation, according to standard protocols. RNA concentration and integrity were determined spectrophotometrically and electrophoretically, respectively. Two micrograms of the isolated RNA was treated with RQ1 DNase (Promega) and used for cDNA synthesis with the M-MLV reverse transcriptase (Promega) according to the manufacturer's instruction. Viral load was determined by detection of the IAV NS1 RNA in the right lungs by real-time quantitative PCR with iTaq Universal SYBR® Green Supermix (Biorad). with primers published elsewhere (Brandes et al. 2013) [5′-3′ Fwd: TGTCAAGCTTTCAGGTAGATTG, Rev: CTCTTAGGGATTTCTGATCTC]. Relative amounts of RNA expression were normalized to Gapdh [5′-3′ Fwd: AGGTGGTCTCCTCTGACTTC, Rev: CTGTTGCTGTAGCCAAATTCG], and calculated according to the DDCT method. Virus RNA quantities in lungs were expressed as fold change relative to age-matched 1-day post infection neonatal mice.

Quantitative reverse transcription (RT)-PCR. At different points during infection, the right lobes of infected lungs were harvested and immediately homogenized in TRIzol (Invitrogen). Total RNA purification was carried out using the RiboPure kit (AB). Conversion into cDNA used the TaqMan RNA-to-CTT 2-step kit (AB). TaqMan quantitation of IFNβ1, SOD3, GSS, GPX3, PRDX1, and GAPDH was carried out with inventoried primers in an AB 7900HT sequence detection system according to the manufacturer's instructions. For relative quantitation of the different mRNA species, all values were normalized to measured levels of GAPDH transcripts and expressed relative to values for uninfected WT mice using the comparative threshold cycle (C_T) method (Applied Biosystems, Guide to performing relative quantitation of gene expression using real-time quantitative PCR).

Isolation of leukocytes. Pulmonary leukocytes were isolated from individual mice by removing lungs and mincing into smaller pieces. The tissue was then digested for two hours at 37 °C with 3.0 mg/ml collagenase A and 0.15 µg/ml DNase I (Roche) in RPMI 1640 (Mediatech) containing 5% heat-inactivated FBS (Life Technologies), 2 mM l-glutamine, 100 IU/ml penicillin, and 100 µg/ml streptomycin (Mediatech). The digested tissue was then passed through a 40-µm cell strainer (Falcon) and washed in the same media as above. Cells were counted using trypan blue exclusion with light microscopy. Bronchoalveolar lavage was obtained by instilling the lungs with 0.1 mL (neonates) or 0.5 mL (adults) PBS/EDTA (25 mM) 5 times via intratracheal cannulation. The samples were centrifuged to obtain cells for flow cytometry.

Isolation of type II epithelial cells. The lungs of neonatal and adult mice were instilled to capacity with Dispase II (ThermoFisher) via a tracheal catheter (29 gauge for neonates, 18 gauge for adults) followed by 0.1% low-melt agarose. Lungs were removed from the animals and digested in Dispase II for two hours at 37 °C. The cell suspension was filtered through progressively smaller cell strainers (100 µm, 40 µm, 25 µm). Leukocytes were depleted from the filtered Type II epithelial cells (TIIECs) by plating the cell suspension on a culture dish coated with purified monoclonal rat anti-mouse anti-CD16/CD32 and anti-CD45 (BD, San Diego, CA) for two hours at 37 °C 10% CO_2. After this enrichment process, we consistently attained >80% purity of TIIECs from neonatal animals (Supplementary Fig. 7).

Flow cytometry. Cells were co-stained with anti-mouse CD45 conjugated to PerCP Cy5.5 (ThermoFisher), anti-mouse CD11b conjugated to APC (BioLegend), anti-mouse CD11c conjugated to PE-eF610 (BioLegend), anti-mouse Ly6G conjugated to Pacific Blue (BioLegend), anti-mouse Ly6C conjugated to AlexaFluor 488 (BioLegend), anti-mouse F4/80 conjugated to Brilliant Violet 605 (BioLegend), and anti-mouse MHC II conjugated to AlexaFluor 700 (BioLegend). To assess the purity of TIIEC ($CD45^-$, $CD324^-$, $CD326^+$, MHC II^+), the cell suspension was stained with CD45 conjugated to PerCP Cy5.5 (ThermoFisher), CD324 conjugated to PE (BioLegend), CD326 conjugated to APC (BioLegend), and MHC II conjugated to FITC (BioLegend). All stains were completed on ice to prevent internalization. All absolute cell numbers are calculated per 100 mg of lung tissue. Cells were fixed in 1% paraformaldehyde (Fisher Scientific) before flow cytometric analysis. Data were collected on a FACS Fortessa using FACS Diva software (BD Biosciences). Analysis was performed using FlowJo software (Tree Star).

Histopathology. Both lobes of the lung were inflated and fixed with 0.5 mL of 4% neutral-buffered formalin solution. Deparaffinized sections from fixed lungs were stained with hematoxylin and eosin (H&E). Lung pathology was scored blindly by a board-certified pathologist. A percentage score was determined for percentage of lung which exhibited alveolitis: 0: 0%, 1: 1–5%, 2: 6–20%, 3: 21–40%, 4: 41–70%, 5: >70%. The same percentage score was determined for peribronchiolitis. Next, an intensity score was determined by counting the number of cells in the most affected alveoli: 0: no cells, 1: 1–5 cells, 2: 6–20 cells, 3: 21–40 cells, 4: 41–70 cells, 5: >70 cells. The same intensity score was determined for cellular infiltration in the bronchioles. A weighted severity score was then determined using these percentage and intensity scores.

Detection of oxidative stress by flow cytometry. For the analysis of oxidative stress via flow cytometry, 1.0×10^6 cells were treated with saline or 2 mM n-acetylcysteine or 400 µM TBHP or 1000 units of IFNβ at 37 °C 10% CO_2 for 1 h in culture media. Cells were then stained with 500 nM CellROX Deep Red diluted in DMSO at 37 °C 10% CO_2 for 30 minutes in culture media. During the last 15 minutes of CellROX staining, 1 µl of 1 mM SYTOX Blue Dead Cell stain solution in DMSO was added to the media. For samples with multiple color flow cytometry, surface staining was performed immediately following CellROX staining but before SYTOX staining. Cells were fixed in 1% paraformaldehyde. The cells were immediately acquired on a Becton Dickinson LSRII flow cytometer and data was analyzed on FlowJo software (10.7.1).

Detection of reactive oxygen species by flow cytometry. To detect intracellular ROS in neonatal and adult lung cells, the Dihydroethidium (DHE) assay kit (Abcam, ab236206) was used. Neonatal and adult animals were infected with influenza virus as above and harvested 2 days post infection. Lungs were processed to form a single cell suspension. 1.0×10^6 cells were incubated at 37 °C 5% CO_2 for 1 h with 5 µM of DHE with saline, 20 mM n-acetylcysteine, 10 µM Antimycin A, or 1000 units of IFNβ. Surface staining was performed immediately after DHE staining and acquired on a Becton Dickinson LSRII flow cytometer and data was analyzed with FlowJo software (10.7.1).

Detection of oxidative stress by CellInsight CX7. Images were acquired on the CellInsight CX7 high content screening platform, an automated 7-channel confocal microscope. Type II pulmonary epithelial cells were stained with a nuclear stain (blue, DAPI, 386 nm), cell membrane stain WGA (red, 647 nm), and CellROX, a marker for reactive oxygen species (green, 488 nm). Ten fields were imaged in each condition. These images were acquired at 10X with a fixed exposure time of 0.1 seconds. Following acquisition, images were analyzed quantitatively using HCS Studio software. Each image had donor-specific manual alterations in Image Settings to correct background. The nuclear stain was gated by area (Object.Area.Ch1) and the oxidative stress stain was gated by area (ObjectCh2.Area.Ch2) and average intensity (ObjectCh2.AvgIntensity.Ch2). The colocalization had a focal channel of DAPI and a target channel of CellROX (Supplementary Table 1**)**.

After scanning the plate, the DAPI/CellROX colocalization was quantified by average intensity (Mean_ROI_A_Target_1_AvgIntensity) which depicted the average intensity of CellROX stain over DAPI staining. The total cell count per condition was enumerated from the DAPI object count, and the average intensity per cell was summed for each condition. Then, the average intensity per cell was calculated by dividing the summed intensity value by the total cell count per condition.

Statistics. Statistical analysis was performed using the Shapiro-Wilk W test for normality, Student's *t*-test and nonparametric Wilcoxon signed-rank test for paired and unpaired samples, one-way analysis of variance (ANOVA) when comparing the means of multiple groups, or log-rank (Mantel–Cox) test for survival curves. Analyses were performed with the GraphPad Prism 9 statistical analysis program. P values < 0.05 were considered to be statistically significant.

Study approval. All experimental procedures and handling of mice were approved by the Drexel University College of Medicine Institutional Animal Care and Use Committee (IACUC), protocol number 20607, project number 1044999. All work was conducted in compliance with government regulations including the US Animal Welfare Act (Animal Welfare Assurance number A3222-01) and the Public Health Service Policy on Humane Care and Use of Laboratory Animals. The Animal Care and Use program at Drexel has received Full Accreditation from AAALAC International.

REFERENCES

1. Resch, B., Kurath-Koller, S., Eibisberger, M. & Zenz, W. Prematurity and the burden of influenza and respiratory syncytial virus disease. *World J. Pediatr.* **12**, 8–18 (2016).
2. Dawood, F. S. et al. Burden of seasonal influenza hospitalization in children, United States, 2003 to 2008. *J. Pediatr.* **157**, 808–814 (2010).
3. Siegrist, C. A. Neonatal and early life vaccinology. *Vaccine* **19**, 3331–3346 (2001).
4. Mohr, E. & Siegrist, C. A. Vaccination in early life: standing up to the challenges. *Curr. Opin. Immunol.* **41**, 1–8 (2016).
5. Adkins, B., Leclerc, C. & Marshall-Clarke, S. Neonatal adaptive immunity comes of age. *Nat. Rev. Immunol.* **4**, 553–564 (2004).
6. Yu, J. C. et al. Innate immunity of neonates and infants. *Front Immunol.* **9**, 1759 (2018).
7. Ogra, P. L., Welliver, R. C., Riepenhoff-Talty, M. & Faden, H. S. Interaction of mucosal immune system and infections in infancy: implications in allergy. *Ann. Allergy* **53**, 523–534 (1984).
8. Wilcox, D. R., Folmsbee, S. S., Muller, W. J. & Longnecker, R. The Type I interferon response determines differences in choroid plexus susceptibility between newborns and adults in herpes simplex virus encephalitis. *MBio* **7**, e00437–00416 (2016).
9. McNab, F., Mayer-Barber, K., Sher, A., Wack, A. & O'Garra, A. Type I interferons in infectious disease. *Nat. Rev. Immunol.* **15**, 87–103 (2015).
10. Jewell, N. A. et al. Differential type I interferon induction by respiratory syncytial virus and influenza a virus in vivo. *J. Virol.* **81**, 9790–9800 (2007).
11. Bogunovic, D. Type I interferons in newborns-neurotoxicity versus antiviral defense. *MBio* **7**, e00639–16 (2016).
12. Crotta, S. et al. Type I and type III interferons drive redundant amplification loops to induce a transcriptional signature in influenza-infected airway epithelia. *PLoS Pathog.* **9**, e1003773 (2013).
13. Davidson, S., Crotta, S., McCabe, T. M. & Wack, A. Pathogenic potential of interferon alphabeta in acute influenza infection. *Nat. Commun.* **5**, 3864 (2014).
14. Davidson, S. et al. IFNlambda is a potent anti-influenza therapeutic without the inflammatory side effects of IFNalpha treatment. *EMBO Mol. Med.* **8**, 1099–1112 (2016).
15. Durbin, J. E. et al. Type I IFN modulates innate and specific antiviral immunity. *J. Immunol.* **164**, 4220–4228 (2000).
16. Durbin, J. E. et al. The role of IFN in respiratory syncytial virus pathogenesis. *J. Immunol.* **168**, 2944–2952 (2002).
17. Durbin, R. K., Kotenko, S. V. & Durbin, J. E. Interferon induction and function at the mucosal surface. *Immunol. Rev.* **255**, 25–39 (2013).
18. Arimori, Y. et al. Type I interferon limits influenza virus-induced acute lung injury by regulation of excessive inflammation in mice. *Antivir. Res.* **99**, 230–237 (2013).
19. Klinkhammer, J. et al. IFN-lambda prevents influenza virus spread from the upper airways to the lungs and limits virus transmission. *Elife* **7**, e33354 (2018).
20. Galani, I. E. et al. Interferon-lambda mediates non-redundant front-line antiviral protection against influenza virus infection without compromising host fitness. *Immunity* **46**, 875–890 e876 (2017).
21. Lazear, H. M. & Diamond, M. S. New insights into innate immune restriction of West Nile virus infection. *Curr. Opin. Virol.* **11**, 1–6 (2015).
22. Wack, A., Terczynska-Dyla, E. & Hartmann, R. Guarding the frontiers: the biology of type III interferons. *Nat. Immunol.* **16**, 802–809 (2015).
23. Akaike, T. et al. Pathogenesis of influenza virus-induced pneumonia: involvement of both nitric oxide and oxygen radicals. *Proc. Natl Acad. Sci. USA* **93**, 2448–2453 (1996).
24. Lin, X. et al. The influenza virus H5N1 infection can induce ROS production for viral replication and host cell death in A549 cells modulated by human Cu/Zn superoxide dismutase (SOD1) Overexpression. *Viruses* **8**, 13 (2016).
25. Hosakote, Y. M., Liu, T., Castro, S. M., Garofalo, R. P. & Casola, A. Respiratory syncytial virus induces oxidative stress by modulating antioxidant enzymes. *Am. J. Respir. Cell Mol. Biol.* **41**, 348–357 (2009).
26. Sgarbanti, R. et al. Redox regulation of the influenza hemagglutinin maturation process: a new cell-mediated strategy for anti-influenza therapy. *Antioxid. Redox Signal.* **15**, 593–606 (2011).
27. Knobil, K., Choi, A. M., Weigand, G. W. & Jacoby, D. B. Role of oxidants in influenza virus-induced gene expression. *Am. J. Physiol.* **274**, L134–L142 (1998).
28. Bhattacharya, A. et al. Superoxide dismutase 1 protects hepatocytes from type i interferon-driven oxidative damage. *Immunity* **43**, 974–986 (2015).
29. O'Donovan, D. J. & Fernandes, C. J. Free radicals and diseases in premature infants. *Antioxid. Redox Signal* **6**, 169–176 (2004).
30. Buonocore, G., Perrone, S. & Tataranno, M. L. Oxidative stress in the newborn. *Oxid. Med. Cell. Longev.* **2017**, 1094247 (2017).
31. Perez, M., Robbins, M. E., Revhaug, C. & Saugstad, O. D. Oxygen radical disease in the newborn, revisited: oxidative stress and disease in the newborn period. *Free Radic. Biol. Med.* **142**, 61–72 (2019).
32. Saugstad, O. D. Bronchopulmonary dysplasia-oxidative stress and antioxidants. *Semin Neonatol.* **8**, 39–49 (2003).
33. Kumova, O. K. et al. Lung transcriptional unresponsiveness and loss of early influenza virus control in infected neonates is prevented by intranasal Lactobacillus rhamnosus GG. *PLoS Pathog.* **15**, e1008072 (2019).
34. Carey, A. J. et al. Rapid evolution of the CD8+ TCR repertoire in neonatal mice. *J. Immunol.* **196**, 2602–2613 (2016).
35. Virus interference: I. The interferon. By Alick Isaacs and Jean Lindenmann, 1957. *CA Cancer J Clin* **38**, 280–290 (1988).
36. Ericsson, A. C. et al. The influence of caging, bedding, and diet on the composition of the microbiota in different regions of the mouse gut. *Sci. Rep.* **8**, 4065 (2018).
37. Koerner, I., Kochs, G., Kalinke, U., Weiss, S. & Staeheli, P. Protective role of beta interferon in host defense against influenza A virus. *J. Virol.* **81**, 2025–2030 (2007).
38. Wu, W. et al. Early IFN-beta administration protects cigarette smoke exposed mice against lethal influenza virus infection without increasing lung inflammation. *Sci. Rep.* **12**, 4080 (2022).
39. Yoo, J. K., Baker, D. P. & Fish, E. N. Interferon-beta modulates type 1 immunity during influenza virus infection. *Antivir. Res.* **88**, 64–71 (2010).
40. Drajac, C. et al. Control of IFN-I responses by the aminopeptidase IRAP in neonatal C57BL/6 alveolar macrophages during RSV infection. *Mucosal Immunol.* **14**, 949–962 (2021).
41. Lin, S. J. et al. The pathological effects of CCR2+ inflammatory monocytes are amplified by an IFNAR1-triggered chemokine feedback loop in highly pathogenic influenza infection. *J. Biomed. Sci.* **21**, 99 (2014).
42. La Gruta, N. L., Kedzierska, K., Stambas, J. & Doherty, P. C. A question of self-preservation: immunopathology in influenza virus infection. *Immunol. Cell Biol.* **85**, 85–92 (2007).
43. Terrazas, C. et al. Ly6C(hi) inflammatory monocytes promote susceptibility to Leishmania donovani infection. *Sci. Rep.* **7**, 14693 (2017).
44. Ng, S. L., Teo, Y. J., Setiagani, Y. A., Karjalainen, K. & Ruedl, C. Type 1 conventional CD103(+) dendritic cells control effector CD8(+) T cell migration, survival, and memory responses during influenza infection. *Front. Immunol.* **9**, 3043 (2018).
45. Glennon-Alty, L., Moots, R. J., Edwards, S. W. & Wright, H. L. Type I interferon regulates cytokine-delayed neutrophil apoptosis, reactive oxygen species production and chemokine expression. *Clin. Exp. Immunol.* **203**, 151–159 (2021).
46. Ye, S., Lowther, S. & Stambas, J. Inhibition of reactive oxygen species production ameliorates inflammation induced by influenza A viruses via upregulation of SOCS1 and SOCS3. *J. Virol.* **89**, 2672–2683 (2015).
47. To, E. E. et al. Mitochondrial reactive oxygen species contribute to pathological inflammation during influenza A virus infection in mice. *Antioxid. Redox Signal.* **32**, 929–942 (2020).
48. Casson, C. N. et al. Neutrophils and Ly6Chi monocytes collaborate in generating an optimal cytokine response that protects against pulmonary Legionella pneumophila infection. *PLoS Pathog.* **13**, e1006309 (2017).
49. Mittal, M., Siddiqui, M. R., Tran, K., Reddy, S. P. & Malik, A. B. Reactive oxygen species in inflammation and tissue injury. *Antioxid. Redox Signal.* **20**, 1126–1167 (2014).
50. Zhong, B. et al. Roflumilast reduced the IL-18-induced inflammatory response in fibroblast-like synoviocytes (FLS). *ACS Omega* **6**, 2149–2155 (2021).
51. Amatore, D. et al. Influenza virus replication in lung epithelial cells depends on redox-sensitive pathways activated by NOX4-derived ROS. *Cell Microbiol.* **17**, 131–145 (2015).
52. Denney, L. & Ho, L. P. The role of respiratory epithelium in host defence against influenza virus infection. *Biomed. J.* **41**, 218–233 (2018).
53. Chroneos, Z. C., Sever-Chroneos, Z. & Shepherd, V. L. Pulmonary surfactant: an immunological perspective. *Cell. Physiol. Biochem.* **25**, 13–26 (2010).
54. Sun, F., Xiao, G. & Qu, Z. Isolation of murine alveolar type II epithelial cells. *Bio Protoc.* **7**, e2288 (2017).
55. Corti, M., Brody, A. R. & Harrison, J. H. Isolation and primary culture of murine alveolar type II cells. *Am. J. Respir. Cell Mol. Biol.* **14**, 309–315 (1996).
56. Saugstad, O. D., Ramji, S. & Vento, M. Resuscitation of depressed newborn infants with ambient air or pure oxygen: a meta-analysis. *Biol. Neonate* **87**, 27–34 (2005).
57. Mohamed, T., Abdul-Hafez, A., Gewolb, I. H. & Uhal, B. D. Oxygen injury in neonates: which is worse? hyperoxia, hypoxia, or alternating hyperoxia/hypoxia. *Pulm. Respir. Res.* **7**, 4–13 (2020).
58. Saugstad, O. D. Oxidative stress in the newborn-a 30-year perspective. *Biol. Neonate* **88**, 228–236 (2005).
59. Yamada, Y. et al. Major shifts in the spatio-temporal distribution of lung antioxidant enzymes during influenza pneumonia. *PLoS ONE* **7**, e31494 (2012).
60. Schamberger, A. C. et al. Glutathione peroxidase 3 localizes to the epithelial lining fluid and the extracellular matrix in interstitial lung disease. *Sci. Rep.* **6**, 29952 (2016).

61. Folz, R. J., Abushamaa, A. M. & Suliman, H. B. Extracellular superoxide dismutase in the airways of transgenic mice reduces inflammation and attenuates lung toxicity following hyperoxia. *J. Clin. Investig* **103**, 1055–1066 (1999).
62. Poonyagariyagorn, H. K. et al. Superoxide dismutase 3 dysregulation in a murine model of neonatal lung injury. *Am. J. Respir. Cell Mol. Biol.* **51**, 380–390 (2014).
63. Decharatchakul, N. et al. Association of combined genetic variations in SOD3, GPX3, PON1, and GSTT1 with hypertension and severity of coronary artery disease. *Heart Vessels* **35**, 918–929 (2020).
64. Suliman, H. B., Ryan, L. K., Bishop, L. & Folz, R. J. Prevention of influenza-induced lung injury in mice overexpressing extracellular superoxide dismutase. *Am. J. Physiol. Lung Cell Mol. Physiol.* **280**, L69–L78 (2001).
65. Nencioni, L. et al. Influenza A virus replication is dependent on an antioxidant pathway that involves GSH and Bcl-2. *FASEB J.* **17**, 758–760 (2003).
66. Hernandez-Saavedra, D., Swain, K., Tuder, R., Petersen, S. V. & Nozik-Grayck, E. Redox regulation of the superoxide dismutases SOD3 and SOD2 in the pulmonary circulation. *Adv. Exp. Med Biol.* **967**, 57–70 (2017).
67. Zelko, I. N., Mariani, T. J. & Folz, R. J. Superoxide dismutase multigene family: a comparison of the CuZn-SOD (SOD1), Mn-SOD (SOD2), and EC-SOD (SOD3) gene structures, evolution, and expression. *Free Radic. Biol. Med.* **33**, 337–349 (2002).
68. Lakshminrusimha, S. et al. Superoxide dismutase improves oxygenation and reduces oxidation in neonatal pulmonary hypertension. *Am. J. Respir. Crit. Care Med.* **174**, 1370–1377 (2006).
69. Kim, J. Y., Choi, G. E., Yoo, H. J. & Kim, H. S. Interferon potentiates toll-like receptor-induced prostaglandin D2 production through positive feedback regulation between signal transducer and activators of transcription 1 and reactive oxygen species. *Front. Immunol.* **8**, 1720 (2017).
70. Snelgrove, R. J., Edwards, L., Rae, A. J. & Hussell, T. An absence of reactive oxygen species improves the resolution of lung influenza infection. *Eur. J. Immunol.* **36**, 1364–1373 (2006).
71. Muller, U. et al. Functional role of type I and type II interferons in antiviral defense. *Science* **264**, 1918–1921 (1994).
72. Gruber, C. et al. Homozygous STAT2 gain-of-function mutation by loss of USP18 activity in a patient with type I interferonopathy. *J. Exp. Med.* **217**, e20192319 (2020).
73. Hwang, S. Y. et al. A null mutation in the gene encoding a type I interferon receptor component eliminates antiproliferative and antiviral responses to interferons alpha and beta and alters macrophage responses. *Proc. Natl Acad. Sci. USA* **92**, 11284–11288 (1995).
74. Cormier, S. A. et al. Limited type I interferons and plasmacytoid dendritic cells during neonatal respiratory syncytial virus infection permit immunopathogenesis upon reinfection. *J. Virol.* **88**, 9350–9360 (2014).
75. Remot, A. et al. Flt3 ligand improves the innate response to respiratory syncytial virus and limits lung disease upon RSV reexposure in neonate mice. *Eur. J. Immunol.* **46**, 874–884 (2016).
76. Soucy-Faulkner, A. et al. Requirement of NOX2 and reactive oxygen species for efficient RIG-I-mediated antiviral response through regulation of MAVS expression. *PLoS Pathog.* **6**, e1000930 (2010).
77. Kelkka, T. et al. Reactive oxygen species deficiency induces autoimmunity with type 1 interferon signature. *Antioxid. Redox Signal.* **21**, 2231–2245 (2014).
78. To, E. E. et al. Endosomal NOX2 oxidase exacerbates virus pathogenicity and is a target for antiviral therapy. *Nat. Commun.* **8**, 69 (2017).
79. To, E. E. et al. Novel endosomal NOX2 oxidase inhibitor ameliorates pandemic influenza A virus-induced lung inflammation in mice. *Respirology* **24**, 1011–1017 (2019).
80. Mendoza, J. L. et al. The IFN-lambda-IFN-lambdaR1-IL-10Rbeta complex reveals structural features underlying type III IFN functional plasticity. *Immunity* **46**, 379–392 (2017).
81. Ank, N. et al. An important role for type III interferon (IFN-lambda/IL-28) in TLR-induced antiviral activity. *J. Immunol.* **180**, 2474–2485 (2008).
82. Salka, K. et al. Innate IFN-lambda responses to dsRNA in the human infant airway epithelium and clinical regulatory factors during viral respiratory infections in early life. *Clin. Exp. Allergy* **50**, 1044–1054 (2020).
83. Medici, T. C. & Radielovic, P. Effects of drugs on mucus glycoproteins and water in bronchial secretion. *J. Int. Med. Res.* **7**, 434–442 (1979).
84. Kerksick, C. & Willoughby, D. The antioxidant role of glutathione and N-acetyl-cysteine supplements and exercise-induced oxidative stress. *J. Int Soc. Sports Nutr.* **2**, 38–44 (2005).
85. Sun, S. Y. N-acetylcysteine, reactive oxygen species and beyond. *Cancer Biol. Ther.* **9**, 109–110 (2010).
86. Zhang, R. H. et al. N-acetyl-l-cystine (NAC) protects against H9N2 swine influenza virus-induced acute lung injury. *Int. Immunopharmacol.* **22**, 1–8 (2014).
87. Geiler, J. et al. N-acetyl-L-cysteine (NAC) inhibits virus replication and expression of pro-inflammatory molecules in A549 cells infected with highly pathogenic H5N1 influenza A virus. *Biochem. Pharmacol.* **79**, 413–420 (2010).
88. Borowski, A. B. et al. Memory $CD8^+$ T cells require CD28 costimulation. *J. Immunol.* **179**, 6494–6503 (2007).
89. Ward, C. L. et al. Design and performance testing of quantitative real time PCR assays for influenza A and B viral load measurement. *J. Clin. Virol.* **29**, 179–188 (2004).

ACKNOWLEDGEMENTS

This work was supported by NIH R01AI149801 to AJC, NIH K08AI108791 to AJC, NIH-DA039005 to PJG, NIH-DA049227 to PJG. The authors would like to thank Alexis Brantly for assisting with CX7 image processing.

AUTHOR CONTRIBUTIONS

O.K.K., P.D.K., and A.J.C. designed the experiments. O.K.K. and A.R. performed the W.T. and IFNαβR$^{-/-}$ experiments, including colony maintenance and flow cytometry. O.K.K. and A.J.C. analyzed data and performed the statistical analyses. I.E.G. and V.T. performed W.T. and IFNαβR$^{-/-}$, Ifnlr1$^{-/-}$ and IFNαβR$^{-/-}$ Ifnlr1$^{-/-}$ survival experiments. O.K.K., H.J., and S.M.M. performed CellInsight CX7 high content screening. J.P. contributed to histology analyses and scoring. P.J.G., E.A., and P.D.K. provided technical support and guidance. O.K.K. and A.J.C. wrote the manuscript.

COMPETING INTERESTS

The authors declare no competing interests.

ADDITIONAL INFORMATION

Supplementary information The online version contains supplementary material available at https://doi.org/10.1038/s41385-022-00576-x.

Correspondence and requests for materials should be addressed to Alison J. Carey.

Reprints and permission information is available at http://www.nature.com/reprints

Publisher's note Springer Nature remains neutral with regard to jurisdictional claims in published maps and institutional affiliations.

Springer Nature or its licensor (e.g. a society or other partner) holds exclusive rights to this article under a publishing agreement with the author(s) or other rightsholder(s); author self-archiving of the accepted manuscript version of this article is solely governed by the terms of such publishing agreement and applicable law.